

**Heterotrophic prokaryote distribution along a 2,300 km
transect in the North Pacific subtropical gyre during a
strong La Niña conditions: relationship between
distribution and hydrological conditions**

**M. GIRAULT¹, H. ARAKAWA², A. BARANI³, H. J. CECCALDI³, F. HASHIHAMA²,
and G. GREGORI³**

[1]{Kanagawa Academy of Science and Technology, LISE 4C-3, 3-25-13 Tonomachi
Kawasaki-ku, Kawasaki-shi, Kanagawa 210-0821, Japan.}

[2]{Department of Ocean Sciences, Tokyo University of Marine Science and Technology,
5-7 Konan 4, Minato-ku, Tokyo 108-8477, Japan.}

[3]{Aix-Marseille Université, Mediterranean Institute of Oceanography MIO UM 110,
Université de Toulon, CNRS/INSU, IRD, 13288, Marseille, cedex 09, France.}

Correspondence to: M. GIRAULT (girault.bmi@gmail.com; gerald.gregori@univ-amu.fr)

Abstract

The spatial distribution of heterotrophic prokaryotes was investigated during the Tokyo–Palau cruise in the western part of the North Pacific subtropical gyre (NPSG) along a north–south transect between 33.60 and 13.25° N. The cruise was conducted in three different hydrological areas identified as the Kuroshio region, the Subtropical gyre area and the Transition zone. Two eddies were crossed along the transect: one cold core cyclonic eddy and one warm core anticyclonic eddy and distributions of the heterotrophic prokaryotes were recorded. By using analytical flow cytometry and a nucleic acid staining protocol, heterotrophic prokaryotes were discriminated into three subgroups depending on their nucleic acid content (low, high and very high nucleic acid contents labeled LNA, HNA and

VHNA, respectively). Statistical analyses performed on the dataset showed that LNA, mainly associated with low temperature and low salinity, were dominant in all the hydrological regions. In contrast, HNA distribution seemed to be associated with temperature, salinity, Chl *a* and silicic acid. A latitudinal increase in the HNA/LNA ratio was observed along the north–south transect and was related to higher phosphate and nitrate concentrations. However, the opposite relationship observed for the VHNA/HNA ratio suggested that the link between nucleic acid content and oligotrophic conditions is not linear, underlying the complexity of the biodiversity in the VHNA, HNA and LNA subgroups. In the Kuroshio Current, it is suggested that the high concentration of heterotrophic prokaryotes observed at station 4 was linked to the path of the cold cyclonic eddy core. In contrast, it is thought that low concentrations of heterotrophic prokaryotes in the warm core of the anticyclonic gyre (Sta. 9) are related to the low nutrient concentrations measured in the seawater column. Our results showed that the high variability between the various heterotrophic prokaryote cluster abundances depend both on the mesoscale structures and the oligotrophic gradient.

1 Introduction

Marine heterotrophic prokaryotes play a key role in pelagic ecosystems both in terms of carbon sequestration and organic matter remineralisation. Their distribution is controlled by biotic (bottom-up control, top-down control by grazing, virus lyses) and abiotic variables (temperature, salinity, pressure, irradiance, nutrient concentrations). These possible limiting variables are shared with the autotrophic community and competition for resources inevitably occurs in order for each to survive in the same pelagic ecosystem. Competition between heterotrophic prokaryotes and phytoplankton for different forms of inorganic nitrogen and phosphorus has been clearly demonstrated both in laboratory experiments and in the open ocean (Currie and Kalff, 1984; Vadstein, 1998; Thingstad et al., 1998). Moreover, several studies have reported that dissolved organic compounds can be an alternative nutrient source for some nutrient-stressed phytoplankton (Duhamel et al., 2010; Girault et al., 2013a). The common utilization of the inorganic and/or organic matter, such as dissolved organic phosphorus, could lead to a tight coupling between the heterotrophic prokaryotes and photoautotrophs along an oligotrophic gradient. However, the relationship between heterotrophic prokaryote abundance and oligotrophic conditions is unclear, especially in terms of mesoscale structures such as eddies (Baltar et al., 2010; Lasternas et

al., 2013). The differences within the same type of mesoscale circulation reported in the literature highlights that the relationship between heterotrophic prokaryotes and photoautotrophs can be dependent on the identification of the different microorganisms making up the community (Girault et al., 2013b).

In this study, using analytical flow cytometry combined with fluorescent dyes, we were able to identify three different subgroups among the bulk of heterotrophic prokaryotes: a group characterized by a very high nucleic acid content (VHNA), another by a high nucleic acid content (HNA), and finally a group with a low nucleic acid content (LNA). Previous studies have reported that the more active microorganisms seem to have the higher nucleic acid contents (Gasol et al., 1999; Lebaron et al., 2001). Complementary results have suggested that heterotrophic prokaryote activities are influenced by environmental parameters especially under oligotrophic conditions (Zubkov et al., 2001; Grégori et al., 2001, 2003a; Nishimura et al., 2005; Sherr et al., 2006; Bouvier et al., 2007). Using the basis of these previous reports, the oligotrophic conditions investigated in the western part of the NPSG during the Tokyo–Palau Cruise enabled us to examine the relationship between different groups of heterotrophic prokaryotes, as defined by different nucleic acid contents, and their environmental conditions.

Investigations into the heterotrophic prokaryote distribution in the western part of the NPSG are scarce and mostly restricted to the Kuroshio Current or the area near the Japan shelf during El-Niño events (Mitbavkar et al., 2009; Kataoka et al., 2009; Kobari et al., 2011). In contrast, the Tokyo Palau cruise was conducted during a strong LaNiña condition and over a large latitudinal gradient to include various seawater masses. In this work, we studied the extent to which abundance and distribution of various heterotrophic prokaryotic groups, defined by flow cytometry (VHNA, HNA, LNA) were influenced by phytoplankton distribution and environmental variables. The relationships between each heterotrophic prokaryote group and two different mesoscale eddies (one anticyclonic and one cyclonic) were also examined in order to identify any modification in organism distribution which could be related to the oligotrophic conditions found during the cruise.

2 Materials and methods

2.1 Study area and sample collection

This study was conducted from 17 January to 8 February 2011 on board RT/V Shinyo Maru during the Tokyo–Palau cruise. Samples were collected in the western part of the NPSG between 33.60 and 13.25° N along the 141.5° E transect (Fig. 1). Twelve stations (Sta.) were sampled using 2.5 L Niskin bottles mounted on a rosette frame equipped with the Conductivity–Temperature–Depth (CTD) and in situ fluorometer system. Seawater was sampled without replicates at several depths between the surface and 200 m. Due to bad weather conditions, the seawater samples between station 1 and 4 were collected only at the surface (3 m) using a single Niskin Bottle. At these 4 stations, expendable Conductivity/Temperature/Depth profiling systems (XCTD) were used to measure temperature and salinity. The Brunt-Väisälä buoyancy frequency (N^2) was calculated using the exact thermodynamic expression reported by King et al. (2012) (equation 1).

$$N^2 = g^2 \left(\frac{d\rho}{dp} - \frac{1}{c_s^2} \right) \quad (1)$$

Where $\frac{d\rho}{dp}$ is the vertical gradient of *in-situ* density (ρ). The acceleration (g) due to the gravity was assumed to be constant during the Tokyo-Palau cruise ($g=9.81$) and the speed of sound (c_s) was calculated depending on the depth, salinity and temperature according to Del Grosso, (1974). The mixed layer depths were estimated as the depths at which the maximum stratification occurred (i.e., maximum of N^2 at each station). The irradiance was monitored at five stations (5, 7, 9, 11, 12) using a Profiling Reflectance radiometer (PRR 600 Biospherical Instrument®). The depth of the euphotic layer was estimated as the depth of 1 % of photosynthetically active radiation at noon.

2.2 Altimetry and large scale climatic conditions

The altimetry data (sea level anomaly) was produced by Ssalto/Duacs and distributed by Aviso, with support from CNES (<http://www.aviso.oceanobs.com/duacs/>). The sea level anomaly map centered on the 18 January 2011 was plotted using the Panoply software from NASA (<http://www.giss.nasa.gov/tools/panoply/>). This map was processed by compiling the data collected over a six weeks period before and after the chosen date (Fig. 1). The current sea maps provided by the bulletin of the Japanese coast guard were used to validate the satellite data and display the paths of both the cyclonic gyre and the Kuroshio Stream (http://www1.kaiho.mlit.go.jp/KANKYO/KAIYO/qboc/index_E.html).

2.3 Nutrient analyses

Nutrient samples were collected from Niskin bottles, immediately put into cleaned plastic tubes in the dark, plunged into liquid nitrogen and stored in the deep freeze (-60°C) until analyses. The highly sensitive colorimetric method incorporating the AutoAnalyzer II (SEAL Analytical) and Liquid Waveguide Capillarity Cells (World precision Instruments), was used to determine nutrient concentrations (nitrate + nitrite, soluble reactive phosphorus and silicic acid) according to the methods listed in Hashihama et al. (2009) and Hashihama and Kanda (2010). Seawater collected at the surface of the western part of NPSG, which had been preserved for > 1 year, was used as nitrate + nitrite blank water. The blank water was analyzed using the chemiluminescent method described in Garside (1982). The detection limits for nitrate + nitrite, soluble reactive phosphorus and silicic acid were 3, 3 and 11 nM, respectively. Because soluble reactive phosphorus consists mainly of orthophosphate and nitrite was not substantially detectable, soluble reactive phosphorus and nitrate + nitrite are hereafter referred to as phosphate and nitrate.

The nutrient fluxes into the surface mixed layer were calculated using the equation $K \frac{dNut}{dz}$ where K is the local vertical diffusivity, Nut the concentration in nutrients (phosphates, nitrates or silicic acid) and $\frac{dNut}{dz}$ the vertical nutrient gradient. To compensate for irregular sampling depths among the stations, the nutrient profiles were linearly interpolated onto the 1 m grid. Then, vertical nutrient gradients were calculated between sequential depth bins (Painter et al., 2013). This method has the advantage to show the nutrient flux from a particular part of the water column. Due to the lack of an Acoustic Doppler Current Profiler (ADCP) on the ship, the local vertical diffusivity (K) was estimated using the literature (Table 1). Among the K values reported in the oligotrophic conditions, a vertical diffusion coefficient of $0.5 \text{ cm}^2 \cdot \text{s}^{-1}$ was chosen as a standard value (Table 1).

2.4 Chlorophyll *a* and flow cytometry analyses

The depth of the deep chlorophyll *a* maximum was determined from fluorescence profiles using the pre-calibrated in situ fluorometer. To measure chlorophyll *a* concentration, 250 cm^3 of seawater was filtrated through Whatman® nucleopore filters (porosity $\sim 0.2 \mu\text{m}$) using a low vacuum pressure ($< 100 \text{ mm of Hg}$). Filters were then immersed into tubes containing N,N-dimethylformamide (DMF)- and stored in the dark at 4°C until analyses on shore.

Chlorophyll a was analysed using a Turner Designs fluorometer pre-calibrated with pure Chl a pigment (Suzuki and Ishimaru, 1990).

Samples for heterotrophic prokaryotes were collected from the Niskin bottles and pre-filtered onto disposable 100 μ m porosity nylon filters to prevent clogging of any in the flow cytometer. Seawater aliquots of 1.8 cm³ were fixed with 2 % (w/v final dilution) formaldehyde solution, quickly frozen in liquid nitrogen and stored in the deep freeze onboard (–60 °C) until analysis at the flow cytometry core facility PRECYM of the Mediterranean Institute of Oceanology (<http://precym.mio.osupytheas.fr>). In the PRECYM, samples were thawed at room temperature and stained using SYBR Green II (Molecular Probes®) methods detailed in Marie et al. (1999), Lebaron et al. (1998) and modified by Grégori et al. (2003b). The analyses were performed on a FACSCalibur flow cytometer (BD Biosciences®) equipped with an air-cooled argon laser (488 nm, 15 mW). For each particle (cell), five optical parameters were recorded: two light scatter signals, namely forward and right angle light scatters and three fluorescences corresponding to emissions in green (515–545 nm), orange (564–606 nm) and red (653–669 nm) wavelength ranges. Data were collected using the CellQuest software (BD Biosciences®) and the analysis and optical resolution of the various groups of heterotrophic prokaryotes were performed a posteriori using the SUMMIT v4.3 software (Beckman Coulter). For each sample, the runtime of the flow cytometer was 2 min and the flow rate set to 50 μ L.min^{–1} (corresponding to the “Med” flow rate of the flow cytometer). TrucountTM calibration beads (Becton Dickinson Biosciences) were also added to the samples just prior to analysis as an internal standard to monitor the instrument stability and accurately determine the volume analyzed. Following the staining of the nucleic acid with SYBR Green II, heterotrophic prokaryotes, excited at 488 nm, were recorded and enumerated according to their right-angle light scatter intensity (SSC) which relates to the cell size and their green fluorescence intensity (515–545 nm) which relates to the nucleic acid content. As already widely described in the literature, several heterotrophic prokaryote groups can be optically resolved by flow cytometry depending on their average green fluorescence intensities related to their nucleic acid content : in this study, a group of cells with a lower green fluorescence corresponding to heterotrophic prokaryotes with a lower nucleic acid content (LNA), a group of cells displaying a higher green fluorescence corresponding to a higher nucleic acid content (HNA) and a last group of cells with the highest green fluorescence intensity corresponding to the highest nucleic acid content (VHNA) (Fig. A1). The overlap between the stained phytoplankton, in particular *Prochlorococcus* and *Synechococcus*, and the heterotrophic prokaryotes (in terms of green fluorescence and side

scatter intensity) was resolved by using red fluorescence (induced by the chlorophyll) to discriminate and identify the photoautotrophs (Sieracki et al., 1995). The heterotrophic prokaryote abundances were also expressed for each cluster (LNA, HNA and VHNA) in terms of carbon biomass using a conversion factor of 15 fg.C.cell⁻¹ (Caron et al., 1995). The carbon biomass was integrated between the surface and the 200 m depth in order to better characterise the upper water column. Although this study focuses on the distribution of the heterotrophic prokaryotes, ultraphytoplankton was also investigated during the Tokyo-Palau project. Briefly, the ultraphytoplankton was sampled thanks to Niskin bottles and filtrated through a 100 µm mesh size. 4.5 cm⁻³ of subsamples preserved with 0.5 cm⁻³ of a 20 % formaldehyde solution (i.e., 2% final concentration) were put into 5 cm⁻³ Cryovials tubes. Similarly to the heterotrophic prokaryote samples, Cryovials tubes were rapidly frozen in liquid nitrogen and stored in a deep freezer (-60 °C) until analysis. Analyses were all performed in the same period than the heterotrophic prokaryotes and based on their light scatter and fluorescence emission properties. Ultraphytoplankton was discriminated in this study into five flow cytometry clusters (*Synechococcus*, *Prochlorococcus*, Picoeukaryotes, Nanoeukaryotes and Nanocyanobacteria-like) as described in Girault et al. (2013b).

2.5 Statistical analysis

To analyse the multivariate data set, principal component analyses (PCA) and redundancy analysis (RDA) were performed using the R software (vegan package) and the Biplot macro for Excel® (Lipkovich and Smith, 2002). PCA was performed in order to qualitatively identify the relationships between heterotrophic prokaryotes and the environmental variables (Pearson, 1901). Possible links between each heterotrophic prokaryote subgroup and their environmental variables were quantitatively examined using the RDA. For the RDA, the data set was log₁₀ (x+1)-transformed to correct for the large differences in scale among the original variables. A Monte-Carlo test was used in order to test the significance of the RDA results. Partial RDAs were also carried out to evaluate the effects of each explanatory variable set on the heterotrophic prokaryote composition (Liu, 1997). The first RDA was performed on the whole data set by taking into account the heterotrophic prokaryotes as one single group. Additional partial RDAs were performed for each subgroup (LNA, HNA, and VHNA). The environmental variables in the additional partial RDAs were classified into three intercorrelated variable groups, namely: the depth-related parameters (phosphate, nitrate, depth), spatial-related parameters (temperature and salinity) and the phytoplankton-related parameters (Chl *a* and silicic acid). This decision was made

considering the results of the PCA (environmental variables were separated into three groups).

3 Results

3.1 Sampling sites and ultraphytoplankton distribution.

The cruise took place along a north–south transect in the western part of the NPSG (141.5° E) during a strong La-Niña climatic event. According to the temperature–salinity diagram presented in the study made by Girault et al. (2013b), three main areas corresponding to the Kuroshio region (Sta. 1–4), the Subtropical gyre (Sta. 5–8) and the Transition zone (Sta. 9–12) were discriminated (Fig. 1). Separation between the Transition zone and the Subtropical gyre was made using the salinity front observed south of station 8. The discrimination between the Kuroshio area and the Subtropical gyre seawater masses was confirmed by comparing the Tokyo-Palau data set and the studies of Sekine and Miyamoto (2002) and Kitajima et al. (2009). The cruise crossed two main eddies identified in this study as a cold core cyclonic eddy (C), and a warm core anticyclonic eddy (A) (Fig. 1). Eddy C (31° N, 141° E) is located in the Kuroshio region and eddy A (20.5° N, 142° E) in the Transition zone. Thanks to the satellite data and daily surface currents of the bulletin of the Japanese coast guard, the creation of the cold core structure was explained by the instability in the meander of the Kuroshio Current between 9 and 12 of July 2010. The cold core was continuously reported all along the cruise. The distribution of the ultraphytoplankton assemblages observed during the Tokyo-Palau cruise was reported in detail in the study of Girault et al., (2013b). Briefly, ultraphytoplankton was characterized by an heterogeneous distribution of its phytoplankton groups associated with the complex distribution of the various seawater masses met during the cruise (including salinity front, subtropical countercurrent, eddies). Among the phytoplankton communities *Prochlorococcus* numerically dominated the ultraphytoplankton assemblages in the samples collected in the stratified oligotrophic areas such as the Subtropical gyre area and the Transition zone. Picoeukaryotes, Nanoeukaryotes and *Synechococcus* also constituted a significant part of the carbon biomass in the region depleted in phosphate and nitrate. The role of the cold core eddy C was reported at the surface where the highest concentration of Nanoeukaryotes in the surface sample was found in the very core of the cyclonic eddy (Sta. 3) and where, the *Synechococcus* outnumbered the *Prochlorococcus* abundance in the path of the cold core

cyclonic eddy (Sta. 4). The Nanocynaobacteria-like group was reported to be controlled by the frontal system observed at station 9 rather than the concentration of inorganic nutrients.

3.2 Stratification of seawater masses and vertical nutrient fluxes

The Brunt-Väisälä buoyancy frequencies calculated from the CTD data set are characterized by low N^2 values ($< 2 \times 10^{-4} \text{ s}^{-2}$) from the surface down to the 90 m depth (Fig. 2). Below this depth, the vertical distribution of N^2 was more irregular and reached at the maximum $1.09 \times 10^{-3} \text{ s}^{-2}$ at station 11 (90 m). Figure 2 also shows that the depth of the N^2 maximum (thermocline depth) tended to be shallower in the southernmost part of the transect (Sta. 1, 185 m to Sta. 11, 90 m) underlying the strengthening of the upper thermocline when the heat flux at the surface is positive and wind mixing is low in the South part of the transect. Along the latitudinal transect, two particular values of the thermocline depths were found at station 3 (145 m) and at station 9 (140 m) corresponding to the cyclonic and anticyclonic eddies, respectively. Moreover, excepted at station 3 and station 9, the first increases of N^2 ($> 2 \times 10^{-4} \text{ s}^{-2}$) from the surface to the 200 m depth corresponded to the depth of the thermocline and indicated the lack of seasonal thermocline as already described in Sprintall and Roemmich (1999). The limit of the euphotic layer (defined by the depth with 1 % of the irradiance at the surface) was also plotted in Figure 2. During the cruise, this limit varied from 84 m (Sta. 7) to 115 m (Sta. 12). Except station 11, the limit of the euphotic layer was located upper the thermocline. The average of the absolute difference between the euphotic layer and the thermocline depths was $34 \pm 11 \text{ m}$.

Figure 3 shows the vertical gradient of nutrients (phosphates, nitrates and silicic acid). The vertical phosphate profiles were characterized by a very low gradient ($< 1 \text{ nM.m}^{-1}$) in the upper 100 m from station 6 to station 12. Both positive and negative gradients were observed and no specific distribution between them was found. Under the depth of 100 m, higher phosphate gradients ($> 3 \text{ nM.m}^{-1}$) were found and defined the phosphacline depths as displayed in Figure 4 of the study made by Girault et al. (2013b). Nitrates showed that vertical profiles closely corresponded to phosphates with negative or positive values lower than 5 nM.m^{-1} and higher gradient below 100 m. The vertical distribution of the silicic acid gradient was more complex with moderate gradients ranging from 0.01 to $0.02 \text{ } \mu\text{M.m}^{-1}$ were observed in the upper 100 m depth at stations 5, 6, 7, and 12. Similarly to phosphates and nitrates, the highest gradients of silicic acid ($0.04 \text{ } \mu\text{M.m}^{-1}$) were found below 100 m depth from station 6 to station 10. Taking into account all the panels of Figure 3, Station 8

showed a particular pattern between 100 m and 160 m depths where two superimposed high gradients were observed. The depths of these high gradients were found to be similar for phosphates and silicic acid (100-115 m and 130-155 m) but the vertical profile of nitrates gradient showed a slightly lower depth (130-140 m and 155-170 m). By using a vertical diffusion coefficient of $0.5 \text{ cm}^2 \cdot \text{s}^{-1}$, the nutrient fluxes were calculated from station 5 to station 11 (Table 2). Phosphate fluxes into the surface mixed layer were negative at stations 5 and 6 (-0.52 and $-1.34 \text{ } \mu\text{mol} \cdot \text{m}^{-2} \cdot \text{d}^{-1}$, respectively) and positive from station 7 to station 11. The positive phosphate fluxes were maximum at station 7 ($9.43 \text{ } \mu\text{mol} \cdot \text{m}^{-2} \cdot \text{d}^{-1}$) and decreased to reach $1.38 \text{ } \mu\text{mol} \cdot \text{m}^{-2} \cdot \text{d}^{-1}$ at station 11. The percentages of diffuse flux per day relative to the standing stock in the mixed layer were particularly low and varied from -0.03% (Sta. 6) to 0.76% (Sta. 8). Nitrate fluxes into the mixed layer were positive and highly variable along the transect (~ 0 to $81.3 \text{ } \mu\text{mol} \cdot \text{m}^{-2} \cdot \text{d}^{-1}$). The percentage of daily diffuse supply relative to the pool reflects this result and varied from ~ 0 (Sta. 7 and 10) to 432% (Sta. 8). The Silicic acid fluxes were globally higher than the phosphate and nitrate fluxes calculated in the mixed layer (up to $571.1 \text{ } \mu\text{mol} \cdot \text{m}^{-2} \cdot \text{d}^{-1}$; Sta. 9). The daily diffuse supply relative to the mixed layer pool was low and spread from 0.002% (Sta. 5) to 0.48% (Sta. 9).

3.3 Distribution of the heterotrophic prokaryotes

After staining with the SYBR green II fluorescent dye, three clusters of heterotrophic prokaryotes were characterized by their different green fluorescence mean intensities (Fig. A1). In the surface samples of the Kuroshio region the average concentrations of LNA, HNA and VHNA were, $8.71 \times 10^5 \pm 3.8 \times 10^5$, $3.27 \times 10^5 \pm 1.4 \times 10^5$ and $2.64 \times 10^5 \pm 1.2 \times 10^5 \text{ cells} \cdot \text{cm}^{-3}$, respectively. In the Subtropical area the average concentrations of LNA, HNA and VHNA were $6.01 \times 10^5 \pm 1.2 \times 10^5$, $2.97 \times 10^5 \pm 1.4 \times 10^5$ and $1.84 \times 10^5 \pm 6.4 \times 10^4 \text{ cells} \cdot \text{cm}^{-3}$, respectively. In the Transition zone the average concentrations of LNA, HNA and VHNA were $5.18 \times 10^5 \pm 1.8 \times 10^5$, $4.38 \times 10^5 \pm 1.6 \times 10^5$ and $1.15 \times 10^5 \pm 6.2 \times 10^5 \text{ cells} \cdot \text{cm}^{-3}$, respectively (Fig. A2). Despite the high variability between the concentrations along the north-south transect, the distribution of the three heterotrophic prokaryote groups was characterized by a common maximum at station 4 and a minimum at station 9. At station 4 the concentrations of LNA, HNA and VHNA were 1.39×10^6 , 5.03×10^5 and $4.35 \times 10^5 \text{ cells} \cdot \text{cm}^{-3}$, respectively. In contrast, the concentrations of LNA, HNA and VHNA at station 9 were 2.07×10^5 , 1.6×10^5 and $5.07 \times 10^4 \text{ cells} \cdot \text{cm}^{-3}$, respectively. To a lesser extent, high concentrations of LNA

($9.13 \times 10^5 \text{ cells.cm}^{-3}$) and HNA ($3.62 \times 10^5 \text{ cells.cm}^{-3}$) were identified at the northernmost station of the Kuroshio region (at station 1).

The vertical distributions of heterotrophic prokaryotes were also investigated along the transect (Fig. 4). As for surface, the vertical distributions of all heterotrophic prokaryote groups are characterized by lower cell concentrations at station 9. In this very station both LNA and HNA concentrations are significantly lower than at the other stations (Kruskal Wallis test, $n = 90$, $P \text{ value} < 0.05$). The LNA cluster is numerically dominant in 99 % of the samples. The VHNA concentrations are lower than the HNA in 75 % of the samples. In term of carbon biomass, the LNA cluster numerically dominated the other clusters from Station 5 to Station 12 (Fig. A3). The latitudinal contribution of the LNA cluster to the total heterotrophic prokaryotes in terms of carbon biomass varied from 47 % (Sta. 9) to 63 % (Sta. 6). Contribution of the HNA cluster is characterized by a low percentage at stations 5 and 6 (22 % and 16 %, respectively) and a near constant contribution between station 7 and the southernmost station 12 ($33 \pm 2 \%$; $n=6$). The contribution of the VHNA cluster was nearly constant from station 5 to 9 ($19 \pm 2 \%$; $n=5$). Then, it reached the lower values in the Transition zone (14 % at Sta. 10, 5 % at Sta.11 and 12 % at Sta.12).

Figure 5a displays the ratios of HNA/LNA concentration depending on depth. In the Kuroshio region, ratios are low and varied from 0.29 (Sta. 2) to 0.44 (Sta. 3). In the Subtropical gyre area, the ratios varied from 0.16 (Sta. 5, 70 m) to 0.82 (Sta. 7, 10 m). The higher ratios (up to 1.03 at Sta. 10, 10 m) were observed in the surface layer of the Transition zone. In the Transition zone and the Subtropical gyre area the higher ratios measured were found between the surface and 100 m. Figure 5b shows the ratio of VHNA/HNA concentrations depending on depth. In the Kuroshio region the ratio varied from 0.53 (Sta. 3) to 1.46 (Sta. 2). In the Subtropical gyre area, the ratio varied from 0.10 (Sta. 7, 58 m) to 1.93 (Sta. 9, 175 m). In the Transition zone the ratio varied from 0.10 (Sta. 12, 70 m) to 1.47 (Sta. 12, 180 m). The average of the VHNA/HNA ratio (0.37 ± 0.35) in the Transition zone was the lowest of the three sampled regions (0.78 ± 0.44 in the Subtropical gyre; 0.88 ± 0.41 in the Kuroshio region).

3.4 Statistical analysis

Results of the Principal Component Analysis (PCA) and the Redundance Analysis (RDA) are shown in Figures 6 and 7, respectively. The correlation circle of the PCA, displays the first two principal components (PC1 and PC2) which accounted for 32.44 and 27.67 % of

the total inertia, respectively. The third and fourth principal components are not shown due to the low inertia exhibited (11 and 8 % of the total inertia, respectively) and the lack of any clear ecological understanding. Silicic acid, Chl *a*, VHNA and LNA were differentiated from temperature and salinity by PC1, while PC2 mainly differentiated depth, nitrate, and phosphate (negative coordinates) from the HNA clusters (positive coordinate). Using hierarchical classification the sampling depths were separated into six different clusters (Table 3 and Fig. 6.) Cluster 1 characterized all the stations located in the Kuroshio region. Cluster 2 corresponded to samples collected at the edge of the Subtropical gyre and contains the deepest sample collected at station 9 (200 m), station in the anticyclone eddy in the transition zone. Samples in Cluster 3 were collected below a depth of 125 m where nitrate and phosphate concentrations were higher than for surface samples. This cluster was defined as the deep layer group. Cluster 4 samples were collected in the center of the subtropical gyre (stations 7 and 8) where heterotrophic prokaryote concentrations were at their maximum in the seawater column. Cluster 5 represented the samples collected in the anticyclonic eddy where a marked salinity has been reported (Girault et al., 2013b). Located in the Transition zone, at the southernmost stations the sixth and last cluster group was characterized by the highest salinity and temperature values. This last cluster (blue dots in the Fig. 6a) is distinguished from the deep layer group (Cluster 3, green dots) by the low nutrient concentrations measured in the upper layer.

A redundancy analysis (Fig. 7) was then performed to find out how the measured environmental factors influenced the distribution of heterotrophic prokaryote subgroups sampled during the cruise. The cumulative percentage of all canonical eigenvalues indicated that 69.1 % of the observed heterotrophic cluster variations were explained by environmental factors. The first two axes of the RDA explained 38 and 24 % of the total variance, respectively. Monte-Carlo tests for these two axes were significant (P value < 0.05 , using 999 permutations) and suggested that environmental parameters might be important in explaining heterotrophic prokaryote distribution. The first axis is negatively correlated with salinity and positively correlated with the LNA cluster. The second axis is negatively correlated with temperature and the HNA cluster and positively correlated with the VHNA cluster. RDA suggested two main correlations between the LNA cluster and the phytoplankton-related variables (Chl *a* and silicic acid) and the HNA cluster with the depth-related variables (nutrients such as nitrate and phosphate and depth).

To confirm and quantify these possible correlations 4 partial RDAs were also performed: one partial RDA using all the heterotrophic prokaryotes at once and one additional partial

RDA for each heterotrophic prokaryote subgroup (LNA, HNA and VHNA). Results of the partial RDA performed on all the heterotrophic prokaryotes showed that among the six environmental variables measured during the cruise, salinity and temperature statistically contribute for 24 and 7.5 % of the variation of the heterotrophic prokaryotes, respectively. To a lesser extent, phosphate alone explained 3.5 % of the variability, whereas Chl a, nitrate, depth and silicic acid explained only 1.8, 1.7, 1.7 and 0.86 %, respectively. The partial RDAs performed either on LNA, or HNA, or VHNA indicated that environmental parameters can explain 60, 55 and 27 % of the total variance, respectively (Table 4). Partial RDA results showed that the spatial related parameters alone can explain up to 31 % of the variation in the heterotrophic prokaryote distribution. The depth-related parameters explained between 6 and 8 % of the variance and finally the phytoplankton-related group explained a maximum 4 % of the variance in the LNA heterotrophic prokaryotes. As far as the HNA cluster is concerned, the joint variation of the spatial- and phytoplankton-related parameters explained 22 % of the variance.

4 Discussion

4.1 Latitudinal distribution of heterotrophic prokaryotes and interaction with phytoplankton

The heterotrophic prokaryote clusters defined by flow cytometry are distributed according to three main areas corresponding to different seawater masses: (i) the Kuroshio region, where the highest heterotrophic prokaryote concentrations were measured, (ii) the Subtropical gyre and (iii) the Transition zone both characterized by a high variability in the heterotrophic prokaryote concentrations in the seawater column (Figs. 1, 4 and A2). Influence of the seawater masses was also evidenced at the subgroup level, where ratios of heterotrophic prokaryote abundances varied along the latitude (Fig. 5). As a latitudinal partition of the ultraphytoplankton assemblages was also reported in the same region as described in the study of Girault et al., (2013b), heterotrophic prokaryotes-phytoplankton interactions are expected, as already observed in some oligotrophic conditions (Gasol and Duarte, 2000; Gomes et al., 2015). However, “pure” phytoplankton-related parameters such as a bottom up control of the VHNA, HNA, and LNA distributions only accounted for a small fraction (1–4 %) of the explained variations and significantly differed from some previous experiments conducted in oligotrophic conditions (Sherr et al., 2006; Bouvier et al.,

2007; Van Wambeke et al., 2011). The lack of important correlation between such phytoplankton-related parameters and heterotrophic prokaryotes should be nuanced by the high percentage (22 %) of the partial joint variation (spatial- and phytoplankton-related parameters) found for the HNA cluster. It highlighted that phytoplankton-related variables were less important for VHNA and LNA than HNA. This variability may indicate that the species in the HNA cluster better interacted with the phytoplankton than those in the LNA or VHNA clusters. This is in agreement with a study of Gasol et al., (1999). This interaction can be reinforced by the predominant role of the temperature, confirmed by the statistical analysis. Indeed, temperature is known to control the activity of heterotrophic prokaryotes in the NPSG (White et al., 2012). Consequently, the partial RDA evidenced and quantified that: (i) the LNA distribution is mainly explained by temperature and salinity and (ii) HNA distribution is mainly explained by an association of variables (temperature, salinity, Chl *a* and silicic acid) rather than a single environmental factor.

The choice of the association of Chl *a* and silicic acid in the phytoplankton-related cluster was motivated by the PCA and RDA results. Considering the Chl *a* concentration as a proxy of phytoplankton biomass, evidences of local Si depletion associated with blooms of diatoms was reported in the Kuroshio Current area (Hashihama et al., 2014). This study also pointed out that large phytoplankton can be in part controlled by the availability of the silicic acid in this very region. However, the effect of silicic acid on phytoplankton over a larger scale was unexpected, such as the lowest concentrations of phosphate and nitrate reported in the euphotic layer of the western part of the NPSG area (Hashihama et al., 2009, 2014; Girault et al., 2013b). Moreover, Si:N:P stoichiometry identified nitrogen and/or phosphorus to be potential limiting factors during the Tokyo–Palau cruise. As far as the smaller phytoplankton sizes are concerned, the nature and the importance of silicic acid uptakes are still controversial. It is the case in this cruise especially when low concentrations of large silicified organisms were measured. However, a high efficient uptake of silicic acid in the NPSG explained by a regeneration mechanism initiated from the marine bacterial assemblages and/or Si-bioaccumulation in some strains of *Synechococcus* could in part explain the statistical association of Chl *a*-Silicic acid as found in this study and already described in the literature (Bidle and Azam, 1999; Baines et al., 2012; Krause et al. 2012).

4.2 Nutrient fluxes and their biological relevance in a stratified system

In addition to the latitudinal pattern, the hierarchical classification also demonstrated a vertical variation of the heterotrophic prokaryotes distributions during the Tokyo–Palau cruise (Cluster 3; Table 3; Fig. 6). Association of both latitudinal and vertical variations of VHNA, HNA and LNA abundances are uncommon in oligotrophic conditions and it confirmed the complexity of mesoscale structures reported in Aoki et al., (2002) and Van Wanbeke et al. (2011). This stratified environment was particularly well defined by the pronounced thermocline and nutricline and lead to a possible relationship between nutrient concentrations and heterotrophic prokaryotes clusters (Girault et al., 2013b). Although the partial RDA showed that the “pure” depth-related variables poorly explained the total heterotrophic prokaryotes variance (6 - 8 %), the sum of their joint effect can explain more than 26 % of the total variation in the LNA distribution, underlying the differences in nutrient utilisation and requirements at the subgroup levels. From the perspective of nutrients these results also suggested that LNA cluster was less abundant than HNA under low phosphate and nitrate conditions (Fig. 4). This is in contrast with the hypothesis proposed for severely P-limited environments which suggests that inorganic phosphorus can exert more severe physiological constraints on the growth of HNA than LNA (Nishimura et al., 2005; Wang et al., 2007). However, it is important to note that both LNA and HNA clusters are likely to include different strains of microorganisms including species adapted to the warm, which have been shown to have lower minimal P cell quotas (Hall et al., 2008). The link between these warm-adapted species and the cell nucleic acid content is however still unclear and depends on the type of environment (Andrade et al., 2007; Van Wanbeke et al., 2011). According to Andrade et al. (2007), the variation in the HNA/LNA ratio observed suggests that low nutrient conditions favoured HNA cells over LNA cells. This result along with the statistical analysis performed in this study may suggest that HNA species are more warm-adapted than LNA in the Subtropical gyre and Transition zone. Decrease of the VHNA/HNA ratio also suggests that the numerically dominant species with high nucleic acid content (HNA) might be more warm-adapted than the cells with the highest nucleic acid content (VHNA). These contrasting results highlight the complex and non linear link between the cell nucleic acid contents and the various ecological meanings as reported in Bouvier et al., (2007) and Van Wanbeke et al. (2009).

As the PCA and RDA analyses did not integrate the nutrient supplies from the mixed layer, a theoretical estimation of the nutrient inputs was calculated using the Brunt-Väisälä buoyancy frequencies (Tables 1 and 2). The results obtained should obviously be taken with caution, especially for nitrates due to the importance of diazotrophy and to episodic dust

deposition not negligible in the NPSG (Wilson, 2003; Kitajima et al., 2009; Maki et al., 2011). Moreover, the oscillation of positive and negative values in phosphate-depleted condition also pointed out the approximation linked to the limit of detection of the phosphate concentration (3 nM) in the oligotrophic upper layer. At the cruise scale, the comparison between phosphate or silicic acid fluxes and the mixed layer integrated concentration of nutrients suggested that the daily diffuse fluxes were of minor importance to resupply nutrients to the surface. Both phosphate, nitrogen and silicic acid diffuse fluxes were in the range of values reported in oligotrophic conditions (Gasol et al., 2009; Painter et al., 2014). This result emphasizes the important role of the microbial loop to sustain the growth of organisms in the western part of the NPSG. At the local scale (Sta. 8), signature of the subtropical counter current (STCC) was also evidenced by the nutrient fluxes despite no noticeable pattern of observed buoyancy frequency. Due to the various locations of high gradients, utilisation of nutrients was not uniform and indicated that nitrate from the bottom layer could support the growth in the vicinity of the STCC layer. The vertical nitrate input appeared to be important because the association of nitracline with thermocline mathematically maximized the daily flux related to the standing pool. Although, Figure 4 did not evidence particular distribution of heterotrophic prokaryotes close to the STCC layer, integrated heterotrophic prokaryote abundance and carbon biomass of HNA in the Subtropical gyre area were maximum at station 8 (Fig. A3). This result is also observed for the ultraphytoplankton distribution where high concentrations were found at this very station (Girault et al., 2013b). In contrast to the low nutrient fluxes observed at the cruise scale, relationships between the STCC and microbial food web *via* the nutrients fluxes appeared to be an important mechanism to sustain the ecosystem in the very Subtropical pacific gyre area.

4.3 Distribution of heterotrophic prokaryotes and eddies

In oligotrophic conditions, environmental factors controlling the distribution of the heterotrophic prokaryotes have usually been compared for two extreme cases: under and outside the influence of an eddy (Baltar et al., 2010). However, few investigations only have addressed the distribution of heterotrophic prokaryotes along a spatial oligotrophic gradient (Thyssen et al., 2005) or taken into account the age of the eddy (Sweeney et al., 2003; Rii et al., 2007). Among the two notable eddies crossed during the Tokyo–Palau cruise, the cold core mesoscale structure C was found at station 3 (Fig. 6). With a lifespan exceeding 6 months, this cold core eddy was particularly older than common cyclonic eddies generated

1 by the Kuroshio instability as reported by the Japan coast guard data center (~1 month). A
2 six month old cyclonic eddy in the “closed” model can be associated with its decay phase,
3 where intense blooms can be observed but which lack significant diatom abundance (Seki et
4 al., 2001). As the pumping effect and the highest microphytoplankton concentration were
5 found at station 3, the classical biogeochemical properties normally associated with an eddy
6 (i.e. single nutrient pulse, “closed system”) cannot correctly describe the cyclonic eddy
7 encountered during the Tokyo–Palau cruise. This shift between theory and observation was
8 also reported in other oligotrophic areas (Seki et al., 2001; Bidigare et al., 2003;
9 Vaillencourt et al., 2003; Landry et al., 2008). With three stations only (stations 2, 3, and 4),
10 only a snapshot of the eddy effects could be presented and it remains difficult, not to say
11 impossible, to describe further the local effect of the eddy during the cruise. Aware of this
12 limitation, a more complex approach including the path of the eddy associated with multiple
13 nutrient inputs has been purposed to explain the variability in microorganisms as
14 demonstrated by Nencioli et al. (2008). This scenario did match well with the Tokyo-Palau
15 data set, where the cold core of the cyclonic eddy moved to the north-west between
16 December and the sampling time of the cruise. The path of the cold core cyclonic eddy
17 could explain the possible decrease in the nutrient uptake from the bottom layer at station 4
18 and lead to an oligotrophic system dominated by regeneration processes. The high
19 abundance of heterotrophic prokaryotes measured at the edge of the cyclonic eddy could be
20 explained by the high activity in the microbial loop. This activity can be in part enhanced by
21 a more efficient vertical exchange of seawater masses at the periphery rather than at the
22 center of the eddy (Stapleton et al., 2002; Klein and Lapeyre, 2009). Similarly, the
23 numerical dominance of *Synechococcus*, observed only once in the surface samples during
24 the cruise, may be the result of the change in trophic conditions (Girault et al., 2013b).

25 In contrast to the frontal structures reported in the literature (Arístegui and Montero, 2005;
26 Baltar et al., 2009; Lasternas et al., 2013), the second eddy (A) located between the
27 Subtropical gyre and the Transition zone was characterized by the lowest concentrations of
28 heterotrophic prokaryotes found during the cruise. These low concentrations were
29 noticeable for all the clusters (LNA, HNA and VHNA) and suggested that the anticyclonic
30 eddy did not enhance nor limit one particular heterotrophic prokaryote cluster between the
31 surface and the bottom of the thermocline (Fig. 4). The high increase in VHNA and LNA
32 compared to HNA, below the thermocline were uncommon in the meso- and bathypelagic
33 zones of oligotrophic areas where the concentration of HNA and LNA decreased

significantly with depth (Van Wambeke et al., 2011; Yamada et al., 2012). Among the environmental variables apt to influence the ratio of the heterotrophic clusters, increase in nutrient concentrations associated with the sloppy feeding mechanism may partially lead to the high abundance of VHNA observed at the bottom of the euphotic layer, as previously reported by Thyssen et al., (2005). The sloppy feeding hypothesis is ecologically coherent because the limit of the euphotic layer was not coupled with the thermocline, underlying that a part of the organic material produced in surface could be transported below the euphotic layer by vertical migration of organisms, improving the grazing activity.

5 Conclusions

This study along a 2300 km transect in the North Pacific subtropical gyre area during a strong La Niña condition showed that the heterotrophic prokaryote distribution is correlated with three different seawater masses identified as (i) the Kuroshio, (ii) the Subtropical gyre and (iii) the Transition zone. A latitudinal increase in the HNA/LNA ratio was found along the equatorward oligotrophic gradient and suggested different relationships between the various heterotrophic clusters and the environmental variables measured in situ during the cruise. The statistical analyses highlighted that the majority of the heterotrophic prokaryote distribution is explained by temperature and salinity. Nutrients and phytoplankton-related variables had different influences depending on the LNA, HNA and VHNA clusters. LNA distribution is mainly correlated with temperature and salinity while HNA distribution is mainly explained by an association of variables (temperature, salinity, Chl a and silicic acid). During the cruise, two eddies (one cyclonic and one anticyclonic) were crossed. The vertical distributions of LNA, HNA and VHNA were investigated. Based on the current surface map and the microorganism distribution, it is reasonable to form the hypothesis that the high concentration of heterotrophic prokaryotes observed at station 4 was linked to the path of the cold cyclonic eddy core. In contrast, in the warm core of the anticyclonic eddy, lower heterotrophic prokaryote concentrations are suggested to be linked to the low nutrient concentrations. Results described in this study highlight the high variability of each heterotrophic prokaryote cluster defined by their nucleic acid content (LNA, HNA, and VHNA) with regard to the mesoscale structures and the oligotrophic gradient observed in situ within the area of the North Pacific subtropical gyre.

Acknowledgements

1 We thank Captain Akira Noda, crew members of the RT/V Shinyo maru of Tokyo
2 University of Marine Science and Technology, (TUMSAT) for their cooperation at sea. We
3 appreciated the English correction of the manuscript made by Tracy L. Bentley. We thank
4 Yuta Nakagawa and Shinko Kinouchi for their help during the cruise. We are grateful to the
5 PRECYM Flow Cytometry Platform of the Mediterranean Institute of Ocenaography (MIO)
6 for the flow cytometry analyses. We also thank the Société franco-japonaise
7 d'Océanographie for its support in shipping the samples from Japan to France.

References

- Andrade, L., Gonzalez A. M., Rezende, C. E., Suzuki, M., Valentin, J. L., and Paranhos, R.: Distribution of HNA and LNA bacterial groups in the Southwest Atlantic Ocean, *Braz. J. Microbiol.*, 38, 330-336, 2007.
- Aoki, Y., Suga, T., and Hanawa, K.: Subsurface subtropical fronts of the North Pacific as inherent boundaries in the ventilated thermocline, *J. Phys. Oceanogr.*, 32, 2299–2311, 2002.
- Arístegui, J. and Montero, M. F.: Temporal and spatial changes in plankton respiration and biomass in the Canary Islands region: the effect of mesoscale variability, *J. Mar. Syst.*, 54, 65–82, 2005.
- Baines, S. B., Twining, B. S., Brzezinski, M. A., and Nelson, D. M.: An unexpected role for picocyanobacteria in the marine silicon cycle, *Nature Geosci.*, 5, 886–891, 2012.
- Baltar, F., Arístegui, J., Montero, M. F., Espino, M., Gasol, J. M., and Herndl, G. J.: Mesoscale variability modulates seasonal changes in the trophic structure of nano- and picoplankton communities across the NW Africa-Canary Islands transition zone, *Prog. Oceanogr.*, 83, 180–188, 2009.
- Baltar, F., Arístegui, J., Gasol, J. M., Lekunberri, I., and Herndl, G. J.: Mesoscale eddies: hotspots of prokaryotic activity and differential community structure in the ocean, *ISME J.*, 4, 975–988, 2010.
- Bidigare, R. R., Benitez-Nelson, C., Leonard, C. L., Quay, P. D., Parsons, M. L., Foley, D. G., and Seki, M. P.: Influence of a cyclonic eddy on microheterotroph biomass and carbon export in the Lee of Hawaii, *Geophys. Res. Letters*, 30, 51, 1-4, 2003.
- Bidle, K. D. and Azam F.: Accelerated dissolution of diatom silica by marine bacterial assemblages, *Nature*, 397, 508-512, 1999.
- Bouvier, T., del Giorgio, P. A., and Gasol, J. M.: A comparative study of the cytometric characteristics of high and low nucleic-acid bacterioplankton cells from different aquatic ecosystems, *Environ. Microbiol.*, 9, 2050–2066, 2007.
- Caron, D. A., Dam, H. G., Kremer, P., Lessard, E. J., Madin, L. P., Malone, T. C., Napp, J. M., Peele, E. R., Roman, M. R., and Youngbluth, M. J.: The contribution of microorganisms to particulate carbon and nitrogen in surface waters of the Sargasso Sea near Bermuda, *Deep-Sea Res. I*, 42, 943–972, 1995.

1 Currie, D. J. and Kalff, J.: Can bacteria outcompete phytoplankton for phosphorus? A
2 chemostat test, *Microb. Ecol.*, 10, 205-216, 1984.

3 Del Grosso, V. A.: New equation for the speed of sound in natural waters with comparisons
4 to other equations, *J. Acoust. Soc. Am.* 56, 1084–1091, 1974.

5 Duhamel, S., Dyhrman, S. T., and Karl, D. M.: Alkaline phosphatase activity and regulation
6 in the North Pacific Subtropical Gyre, *Limnol. Oceanogr.*, 55, 1414–1425, 2010.

7 Emerson, S., Quay, P. D., Stump, C., Wilbur, D., and Schudlich, R.: Chemical tracers of
8 productivity and respiration in the subtropical Pacific Ocean, *J. Geophys. Res.*, 100, 15873-
9 15887, 1995.

10 Garside, C.: A chemiluminescent technique for the determination of nanomolar
11 concentrations of nitrate and nitrite in seawater, *Mar. Chem.*, 11, 159–167, 1982.

12 Gasol J. M. and Duarte, C. M.: Comparative analyses in aquatic microbial ecology: how far
13 do they go? *FEMS Microbiol. Ecol.*, 31, 99-106, 2000.

14 Gasol J. M., Zweifel, U. L., Peters, F., Fuhrman, J. A., and Håggström, A.: Significance of
15 size and nucleic acid content heterogeneity as measured by flow cytometry in natural
16 planktonic bacteria, *App. Environ. Microbiol.*, 65, 4475–4483, 1999.

17 Gasol J. M., Vázquez-Domínguez, E., Vaqué, D., Agustí, S., and Duarte, C. M.: Bacterial
18 activity and diffuse nutrient supply in the oligotrophic central Atlantic Ocean, *Aquat.*
19 *Microb. Ecol.*, 56, 1-12, 2009.

20 Girault, M., Arakawa, H., and Hashihama, F.: Phosphorus stress of microphytoplankton
21 community in the western subtropical North Pacific, *J. Plankton Res.*, 35, 146-157, 2013a.

22 Girault, M., Arakawa, H., Barani, A., Ceccaldi, H. J., Hashihama, F., Kinouchi, S., and
23 Grégori, G.: Distribution of ultraphytoplankton in the western part of the North Pacific
24 subtropical gyre during a strong La Niña condition: relationship with the hydrological
25 conditions, *Biogeosciences*, 10, 5947-5965, 2013b.

26 Gomes, A., Gasol J. M., Estrada, M., Franco-Vidal, L., Díaz-Pérez, L., Ferrera I., Anxelu,
27 and Morán, X.: Heterotrophic bacterial responses to the winter–spring phytoplankton bloom
28 in open waters of the NW Mediterranean, *Deep-Sea Res. PT I*, 96, 59-68, 2015.

29 Grégori, G., Denis, M., Lefevre, D., and Romano, J. C.: Viability of heterotrophic bacteria
30 in the Bay of Marseilles, *C. R. Biol.*, 326, 739-750, 2003a.

1 Grégori G., Denis, M., Sgorbati, S., and Citterio, S.: Resolution of viable and membrane-
2 compromised free bacteria in aquatic environments by flow cytometry, *Curr. Protoc.*
3 *Cytom.*, 23, 11.15.1–11.15.7, 2003b.

4 Grégori G., Citterio, S., Ghiani A., Labra, M., Sgorbati, S., Brown, S., Denis, M.:
5 Resolution of viable and membrane compromised bacteria in fresh and marine waters based
6 on analytical flow cytometry and nucleic acid double staining, *Appl. Environ. Microbiol.*,
7 67, 4662-4670, 2001.

8 Hall, E. K., Neuhauser, C., and Cotner, J.: toward a mechanistic understanding of how
9 natural bacterial communities respond to changes in teperature in aquatic ecosystems, *ISME*,
10 2, 471–481, 2008.

11 Hashihama, F., Furuya, K., Kitajima, S., Takeda, S., Takemura, T., and Kanda, J.: Macro-
12 scale exhaustion of surface phosphate by dinitrogen fixation in the western North Pacific,
13 *Geoph. Res. Lett.*, 36, L03610, doi:10.1029/2008GL036866, 2009.

14 Hashihama, F. and Kanda, J.: Automated colorimetric determination of trace silicic acid in
15 seawater by gas-segmented continuous flow analysis with a liquid waveguide capillary cell,
16 *La Mer*, 47, 119–127, 2010.

17 Hashihama, F., Kanda, J., Maeda, Y., Ogawa, H., and Furuya, K.: Selective depressions of
18 surface silicic acid within cyclonic mesoscale eddies in the oligotrophic western North
19 Pacific, *Deep-Sea Res. PT I*, 90, 115-124, 2014.

20 Kataoka, T., Hodoki, Y., Suzuki, K., Saito, H., Higashi, S.: Tempo-spatial patterns of
21 bacterial community composition in the western North Pacific Ocean, *J. Marine Syst.*, 77,
22 197-207, 2009.

23 Kitajima, S., Furuya, K., Hashihama, F., Takeda, S., and Kanda, J.: Latitudinal distribution
24 of diazotrophs and their nitrogen fixation in the tropical and subtropical western North
25 Pacific, *Limnol. Oceanogr.*, 54, 537–547, 2009.

26 King, B., Stone , M., Zhang, H. P., Gerkema, T., Marder, M., Scott, R. B. and Swinney, H.
27 L.: Buoyancy frequency profiles and internal semidiurnal tide turning depths in the oceans,
28 *J. Geophys. Res.*, 117, C04008, DOI:10.1029/2011JC007681, 2012.

29 King, F. D., and Devol, A. H.: Estimates of vertical eddy diffusion through the thermocline
30 from phytoplankton nitrate uptake rates in the mixed layer of the estern tropical Pacific.,
31 *Limnol, Oceanogr.*, 24, 645-651, 1979.

1 Klein, P. and Lapeyre G.: The oceanic vertical pump induced by mesoscale and
2 submesoscale turbulence, *Annu. Rev. Mar. Sci.*, 1, 351-375, 2009.

3 Kobari, T., Hijiya, K., Minowa, M., and Kitamura, M.: Depth distribution, biomass and
4 taxonomic composition of subtropical microbial community in southwestern Japan, *South
5 Pacific Studies*, 32, 31-43, 2011.

6 Krause, J. W., Brzezinski, M. A., Villareal, T. A., and Wilson, C.: Increased kinetic
7 efficiency for silicic acid uptake as a driver of summer diatom blooms in the North Pacific
8 subtropical gyre, *Limnol. Oceanogr.*, 57, 1084-1098, 2012.

9 Landry, M. R., Brown, S. L., Rii, Y. M., Selph, K. E., Bidigare, R.R., Yang E.J., and
10 Simmons, M. P.: Depth-stratified phytoplankton dynamics in Cyclone Opal, a subtropical
11 mesoscale eddy, *Deep-Sea Res. PT II*, 56, 1348-1359, 2008.

12 Lasternas, S., Piedeleu, M., Sangrà, P., Duarte, C. M., and Agustí, S.: Forcing of dissolved
13 organic carbon release by phytoplankton by anticyclonic mesoscale eddies in the
14 subtropical NE Atlantic Ocean, *Biogeosciences*, 10, 2129-2143, 2013.

15 Lebaron, P., Parthuisot, N., and Catala, P.: Comparison of blue nucleic acid dyes for flow
16 cytometric enumeration of bacteria in aquatic systems, *Appl. Environ. Microbiol.*, 64, 1725-
17 1730, 1998.

18 Lebaron, P., Servais, P., Agogue, H., Courties, C., and Joux, F.: Does the high nucleic acid
19 content of individual bacterial cells allow us to discriminate between active cells and
20 inactive cells in aquatic systems?, *Appl. Environ. Microbiol.* 67, 1775–1782, 2001.

21 Ledwell, J. R., Watson, A. J., and Laws, C. S.: Mixing of a tracer in the pycnocline, *J.
22 Geophys. Res.*, 103, 21499–21529, 1998.

23 Ledwell, J. R., Mc Gillicuddy Jr., D. J., and Anderson, L. A.: Nutrient flux into an intense
24 deep chlorophyll layer in a mode-water eddy, *Deep-Sea Res. Pt. II*, 55, 1139–1160, 2008.

25 Li, Y.-H., Peng, T.-H., Broecker, W. S., and Göte Östlund H.: The average vertical mixing
26 coefficient for the oceanic thermocline, *Tellus*, 36B, 212-217, 1984.

27 Lipkovich, L. I and Smith, E. P.: Biplot and singular value decomposition macros for
28 Excel®, *J. Stat. Softw.*, 7, 1-15, 2002.

29 Liu, Q.: Variation partitioning by partial redundancy analysis (RDA), *Environmetrics*, 8,
30 75-85, 1997.

1 Maki, T., Ishikawa, A., Kobayashi, F., Kakikawa, M., Aoki, K., Mastunaga, T., Hasegawa
2 H., and Iwasaka, Y.: Effects of Asian dust (KOSA) deposition event on bacterial and
3 microalgal communities in the Pacific Ocean, *Asian Journal of Atmospheric Environment*,
4 5, 157-163, 2011.

5 Marie, D., Brussaard, C. P. D., Thyraug, R., Bratbak, G., and Vaulot, D.: Enumeration of
6 marine viruses in culture and natural samples by flow cytometry, *Appl. Environ. Microbiol.*,
7 65, 45–52, 1999.

8 Mitbavkar, S., Saino, T., Horimoto, N., Kanda, J., and Ishimaru T.: Role of environment
9 and hydrography in determining the picoplankton community structure of Sagami Bay,
10 Japan, *J. Oceanogr.*, 65, 195-208, 2009.

11 Nencioli, F., Dickey, T. D., Kuwahara V. S., Black W., Rii, Y. M., and Bidigare, R. R.:
12 Physical dynamics and biological implications of a mesoscale cyclonic eddy in the Lee of
13 Hawaii: Cyclone Opal observations during E-Flux III, *Deep-Sea Res. PT II*, 55, 1252–1274,
14 2008.

15 Nishimura, Y., Kim, C., and Nagata, T.: Vertical and seasonal variations of
16 bacterioplankton subgroups with different nucleic acid contents: possible regulation by
17 phosphorus, *Appl. Environ. Microbiol.*, 71, 5828-5836, 2005.

18 Painter, S. C., Henson, S. A., Forryan, A., Steigenberger, S., Klar, J., Stinchcombe, M. C.,
19 Rogan, N., Baker, A. R., Achterberg, E. P., and Moore, C. M.: An assessment of the vertical
20 diffusive flux of iron and other nutrients to the surface waters of the subpolar North Atlantic
21 Ocean, *Biogeosciences*, 11, 2113-2130, 2014.

22 Pearson, K.: On lines and planes of closest fit to systems of points in space, *Philos. Mag.*, 2,
23 559–572, 1901.

24 Rii, Y. M., Brown Susan, L., Nencioli, F., Kuwahara, V., Dickey, T., Karl D. M., and
25 Bidigare, R. R.: The transient oasis: Nutrient-phytoplankton dynamics and particle export in
26 Hawaiian lee cyclones, *Deep-Sea Res. PT II*, 55, 1275–1290, 2008.

27 Rooth, C., and Ostlund H. G.: Penetration of tritium into the Atlantic thermocline, *Deep-Sea*
28 *Res.* 19, 481-492, 1972.

29 Seki, M. P., Polovina, J. J., Brainard, R. E., Bidigare, R. R., Leonard, C. L., and Foley, D.
30 G.: Biological enhancement at cyclonic eddies tracked with goes thermal imagery in
31 hawaiian waters, *Geophys. Res. Lett.*, 28, 1583–1586, 2001.

1 Sekine, Y. and Miyamoto, S.: Influence of Kuroshio flow on the horizontal distribution of
2 north Pacific intermediate water in the Shikoku basin, *J. Oceanogr.*, 58, 611–616, 2002.

3 Sherr, B., Sherr, E., and Longnecker, K.: distribution of bacterial abundance and cell-
4 specific nucleic acid content in the Northeast Pacific Ocean, *Deep-Sea Res. PT I*, 53, 713–
5 725, 2006.

6 Sieracki, M. E., Haugen, E. M., and Cucci, T. L.: Overestimation of heterotrophic bacteria
7 in the Sargasso Sea: direct evidence by flow and imaging cytometry. *Deep Sea Res. PT I*,
8 42, 1399–1409, 1995.

9 Sprintall, J., and Roemmich, D., Characterizing the structure of the surface layer in the
10 Pacific Ocean, *J. Geophys. Res.*, 104, 23297-23311, 1999.

11 Stapleton, N. R., Aicken, W. T., Dovey, P. R., and Scott, J. C.: The use of radar altimeter
12 data in combination with other satellitesensors for routine monitoring of the ocean: case
13 study of the northern Arabian sea and Gulf of Guam, *Can. J. Remote Sens.*, 28, 567-572,
14 2002.

15 Suzuki, R. and Ishimaru, T.: An improved method for the determination of phytoplankton
16 chlorophyll using N,N-Dimethylformamide, *J. Oceanogr. Soc. Japan*, 46, 190–194, 1990.

17 Sweeney, E. N., McGillicuddy, D. J., and Buesseler, K. O.: Bio- geochemical impacts due
18 to mesoscale eddy activity in the sargasso sea as measured at the bermuda atlantic time-
19 series study (BATS), *Deep Sea Res. PT II*, 50, 3017–3039, 2003.

20 Thingstad T. F., Zweifel, U. L., and Assoulzadegan, F. R.: P-limitation of heterotrophic
21 bacteria and phytoplankton in the north- west Mediterranean, *Limnol. Oceanogr.* 43, 88–94,
22 1998.

23 Thyssen, M., Lefèvre, D., Caniaux, G., Ras, J., Fernández, C. I., and Denis, M.: Spatial
24 distribution of heterotrophic bacteria in the northeast Atlantic (POMME study area) during
25 spring 2001, *J. Geophys Res.*, 110, C07S16, DOI: 10.1029/2004JC002670, 2005.

26 Vadstein, O.: Evaluation of competitive ability of two heterotrophic planktonic bacteria
27 under phosphorus limitation, *Aquatic Microb. Ecol.*, 14, 119-127, 1998.

28 Vaillancourt, R. D., Marra, J., Seki, M. P., Parsons, M. L., and Bidigare, R. R.: Impact of a
29 cyclonic eddy on phytoplankton community structure and photosynthetic competency in the
30 subtropical North Pacific Ocean, *Deep Sea Res. PT I*, 50, 829–847, 2003.

1 Van Scoy, K. A., and Kelley, D. E.: Inferring vertical diffusivity from two decades of
2 tritium penetration, EOS, Trans. AGU., 77, Ocean Sci. Meet. Suppl. OS40, 1996.

3 Van Wambeke, F., Ghiglione, J.-F., Nedoma, J., Mével, G., and Raimbault, P.: Bottom up
4 effects on bacterioplankton growth and composition during summer-autumn transition in
5 the open NW Mediterranean Sea, Biogeosciences, 6, 705-720, doi:10.5194/bg-6-705-2009,
6 2009.

7 Van Wambeke, F., Catala, P., Pujo-Pay, M., and Lebaron, P.: Vertical and longitudinal
8 gradients in HNA-LNA cell abundances and cytometric characteristics in the Mediterranean
9 Sea, Biogeosciences, 8, 1853-1863, DOI: 10.5194/bg-8-1853-2011, 2011.

10 Vernet, M. and Lorenzen, C. J.: The presence of chlorophyll *b* and the estimation of
11 phaeopigments in marine phytoplankton. J. Plankton Res., 9, 265-265, 1987.

12 Wang, H., Smith, H. L., Kuang, Y., and Elser, J. J.: Dynamics of stoichiometric bacteria-
13 algae interactions in the epilimnion, Siam J. Appl. Math., 68, 503–522, 2007.

14 White, A. E., Watkins-Brandt, K. S., Engle, M. A., Burkhardt, B., and Paytan, A.:
15 Characterization of the rate and temperature sensitivities of bacterial remineralization of
16 dissolved organic phosphorus compounds by natural populations. Front. Microbiol., 3, 276,
17 2012.

18 White, W., and Bernstein, R.: Large-scale vertical eddy diffusion in the main pycnocline of
19 the central North Pacific, J. Phys., Oceanogr., 11, 434-441, 1981.

20 Wilson, C.: Late Summer chlorophyll blooms in the oligotrophic North Pacific Subtropical
21 Gyre, Geophys. Res. Lett., 30, 1942, doi:10.1029/2003GL017770, 2003.

22 Yamada N., Fukuda, H., Ogawa, H., Saito, H., and Suzumura, M.: Heterotrophic bacterial
23 production and extracellular enzymatic activity in sinking particulate matter in the western
24 North Pacific Ocean, Front. Microbiol., 3, 379, DOI: 10.3389/fmicb.2012.00379, 2012.

25 Zubkov, M. V., Fuchs, B. M., Burkill, P. H., and Amann, R.: Comparison of cellular and
26 biomass specific activities of dominant bacterioplankton groups in stratified waters of the
27 Celtic Sea, Appl. Environ. Microbiol., 67, 5210–5218, 2001.

1 Table 1. Literature estimates of vertical turbulent diffusivity rates obtained using different
2 methods in the oligotrophic condition. *na* indicates information not mentioned.

Domain	Location	Depth (m)	Diffusivity (cm ² .s ⁻¹)	Reference
North Pacific Subtropical Gyre	22°N-158°W	300-500	0.1-0.5	(Christian and Lewis, 1997)
	35–44°N, 150–170°W	<i>na</i>	0.2-0.4	(White and Berstein, 1981)
	10°N-40°N	0-1000	0.3	(Van Scoy and Kelley, 1996)
	22°N-158°W	<i>Euphotic</i>	1-2	(Emerson <i>et al.</i> , 1995)
Pacific Ocean	20°S-20°N	125	0.5	(Li <i>et al.</i> , 1984)
	20°N-60°N	100	1.8	(Li <i>et al.</i> , 1984)
Tropical North Pacific Ocean	5°N-10°N, 90°E	<i>na</i>	0.05-0.16	(King and Devol, 1979)
	10°N-15°N, 85°E	<i>na</i>	0.44-1.10	(King and Devol, 1979)
Subtropical North Atlantic	25°N, 28°W	300	0.12-0.17	(Ledwell <i>et al.</i> , 1998)
	28.5°N, 23°W	100-400	0.37	(Lewis <i>et al.</i> , 1986)
	31°N, 66°W	<100	0.35	(Ledwell <i>et al.</i> , 2008)

3

1 Table 2. Phosphate, nitrate and silicic acid diffusive fluxes into the surface mixed layer and the importance of supply term relative to the
2 standing pool size.

Station	Latitude	Mixed layer depth (m)	Phosphate flux ($\mu\text{mol.m}^{-2}.\text{d}^{-1}$)	Daily diffusive supply relative to pool (%)	Nitrate flux ($\mu\text{mol.m}^{-2}.\text{d}^{-1}$)	Daily diffusive supply relative to pool (%)	Silicic acid flux ($\mu\text{mol.m}^{-2}.\text{d}^{-1}$)	Daily diffusive supply relative to pool (%)
5	28.98	141	-0.52	-0.01	3.63	0.01	2.25	0.002
6	27.16	136	-1.34	-0.03	12.88	0.04	54.09	0.03
7	24.83	109	9.43	0.69	0	0	142.21	0.21
8	22.83	101	7.78	0.76	81.3	432	351.36	0.39
9	20.78	140	6.48	0.68	13.91	5.7	571.1	0.48
10	19.98	95	1.38	0.16	0	0	0.006	0.01

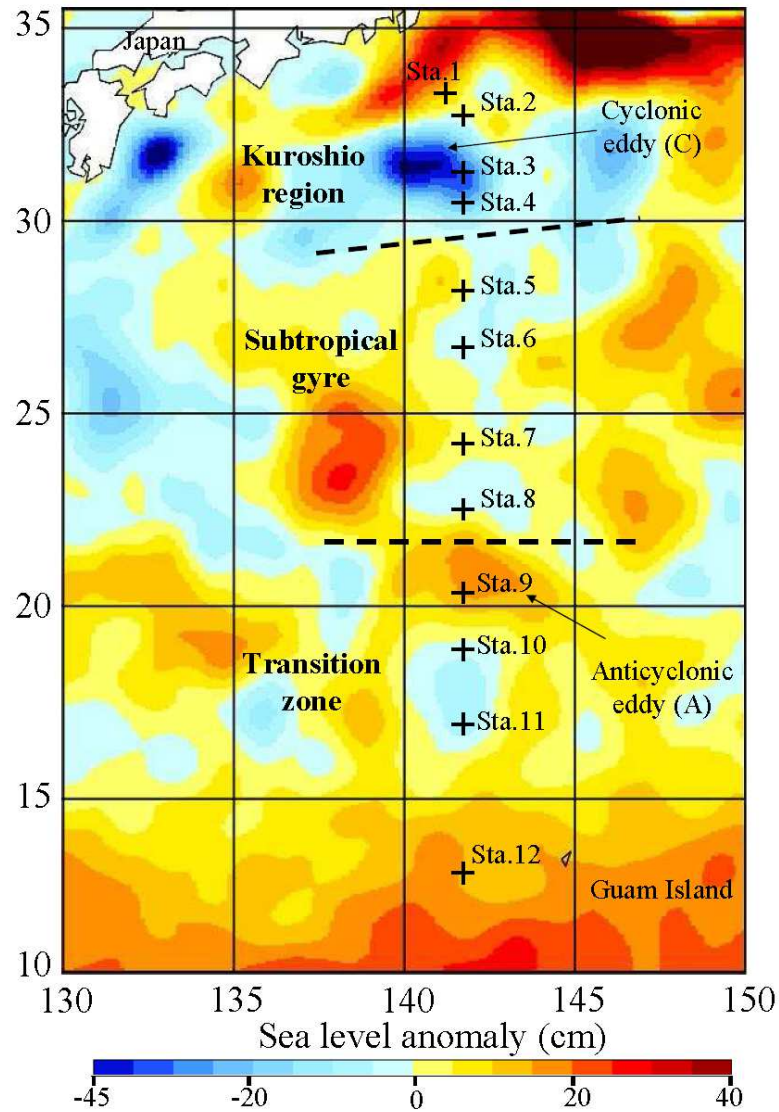
3

Table 3. List of observations from stations 1 to 11 and their classification into six clusters according to the principal component analysis (PCA).

PCA Cluster	Observations	Latitude (°N)	Station	Depth (m)
1	1	33.6	1	0
1	2	33	2	0
1	3	31.6	3	0
1	4	31	4	0
2	5,6,7,8,9,10,11,12,13	28.6	5	0,40,60,70,78,80,100,120,140
2	15,16,17,18,19,20,21,22,23	27.1	6	0,25,60,75,80,90,100,115,125
2	32,33,34	24.5	7	75,90,101
2	40,41	22.5	8	110,125
2	55	20.5	9	200
3	14	28.6	5	160
3	24	27.1	6	150
3	42,43,44	22.5	8	135,150,165
3	54	20.5	9	160
3	61	19.6	10	125
4	25,26,27,28,29,30,31	24.5	7	0,10,25,40,58,59,60
4	35,36,37,38,39	22.5	8	0,25,50,75,95
5	45,46,47,48,49,50,51,52,53	20.78	9	0,25,50,75,100,120,130,140
5	59,60,62	19.6	10	75,100,150
6	56,57,58	19.6	10	0,25,50
6	63,64,65,66	17.2	11	0,30,45,60

Table 4. Partial redundancy analysis performed on each heterotrophic prokaryote cluster optically resolved by flow cytometry: low nucleic acid content (LNA), high nucleic acid content (HNA) and very high nucleic acid content (VHNA). According to the PCA results, Chl *a* and silicic acid are the phytoplankton-related variables. Temperature and salinity are the spatial-related variables. Nitrate, phosphate and depth are the depth-related variables. Negative values characterized the lack of any correlation between heterotrophic prokaryote clusters and the variables tested.

		LNA	HNA	VHNA
Total explained variance		60%	55%	27%
Joint variation	Phytoplankton-related and spatial- and depth-related	6%	-1%	-1%
Partial joint variation	Spatial-related and phytoplankton-related	-1%	22%	-4%
	Spatial- and depth-related	9%	1%	5%
	Depth-related and phytoplankton-related	3%	1%	0%
Unique variation	Phytoplankton-related	4%	1%	1%
	Depth-related	8%	8%	6%
	Spatial-related	31%	23%	20%



1
2 Figure 1: Map of the sea level anomaly (cm) in the west part of the North Pacific
3 subtropical gyre. The sampling stations (black crosses) were separated depending on
4 temperature and salinity into 3 areas: Kuroshio region (stations 1-4), Subtropical gyre
5 (stations 5-8) and the Transition zone (stations 9-12).

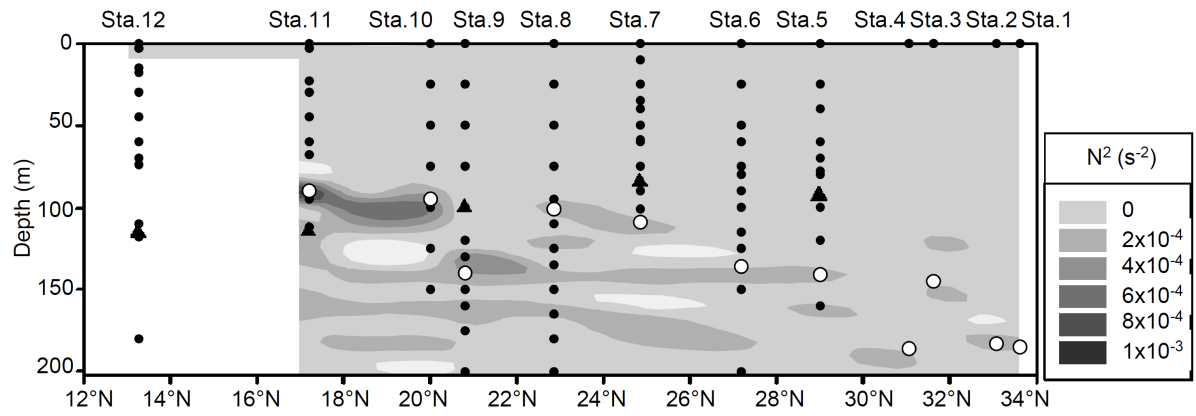


Figure 2: Vertical profiles of the Brunt-Väisälä buoyancy frequency (N^2) calculated from the temperature - salinity measurements. The white circles display the thermocline depth and the black triangles the depths of 1% of photosynthetically active radiation (limit of the euphotic zone).

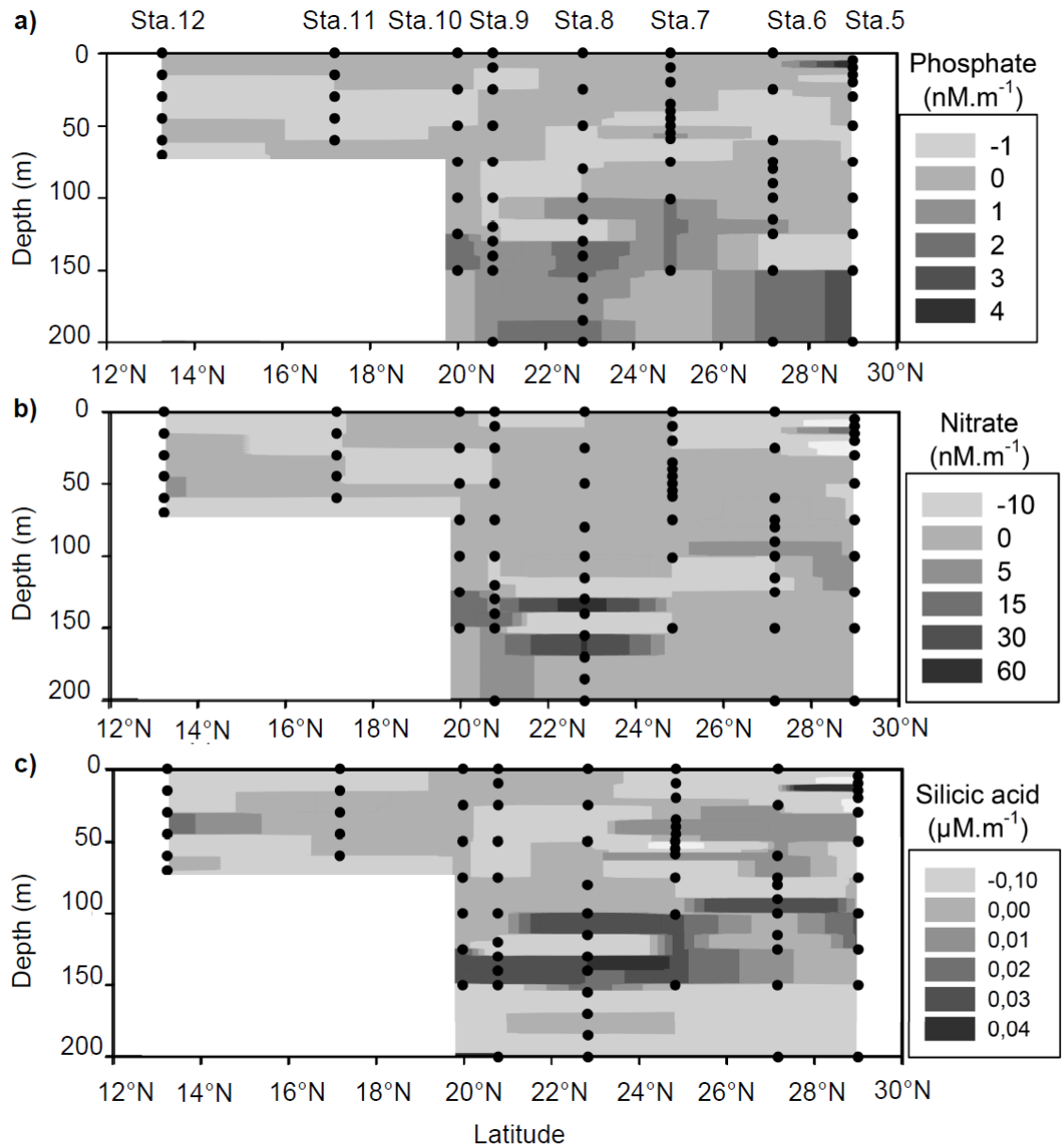


Figure 3: Vertical nutrient gradient ($d\text{Nutrient}/dz$) of Phosphate (a), Nitrate (b) and Silicic acid (c), between station 5 and station 12. The black dots display the sample depths and the names of the stations are indicated in the upper axes.

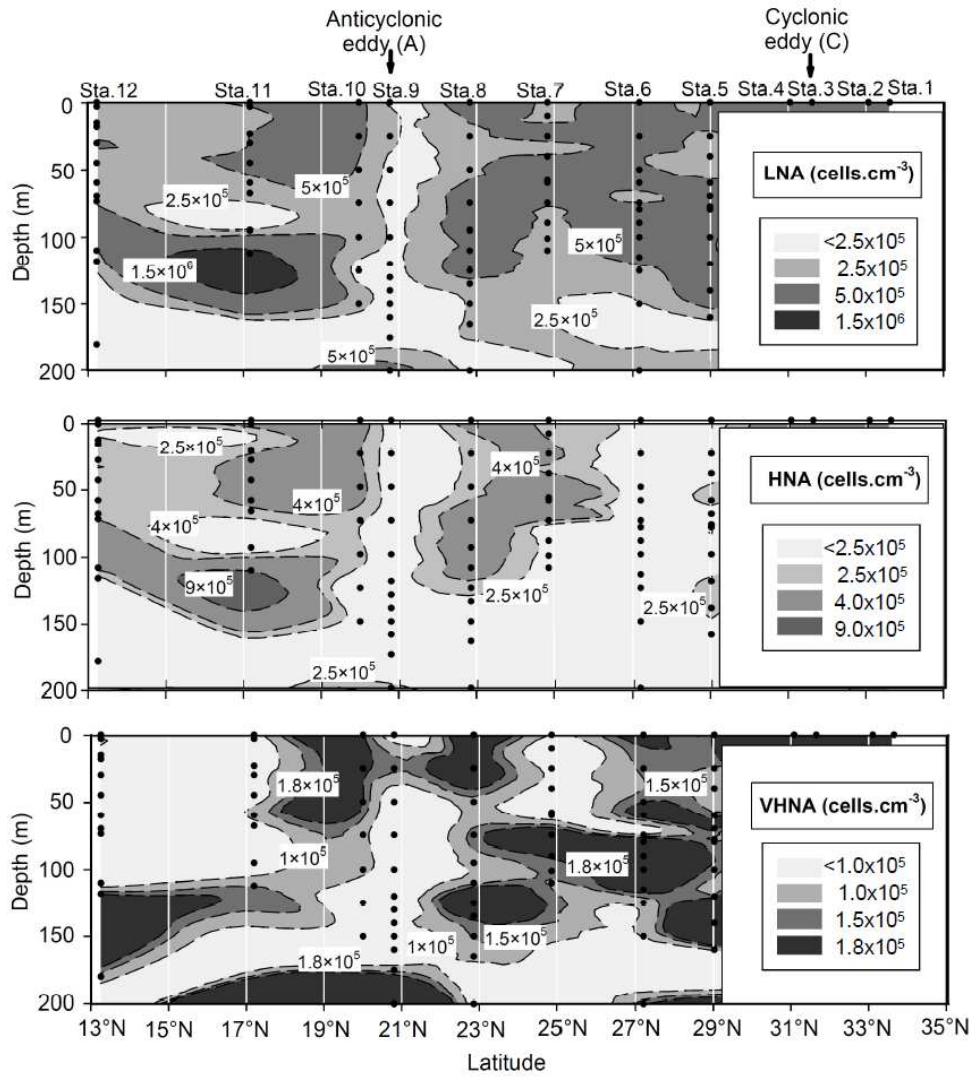
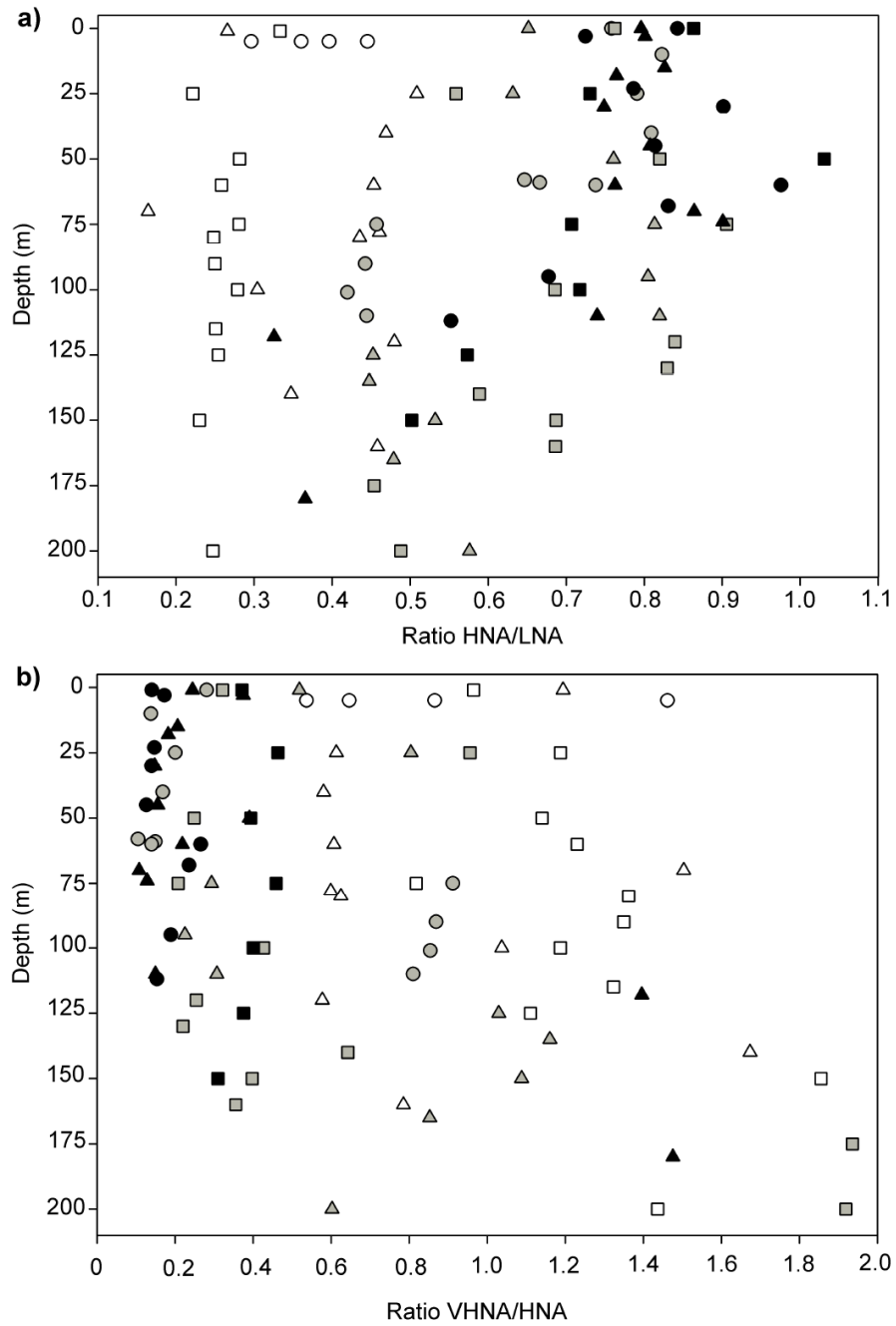
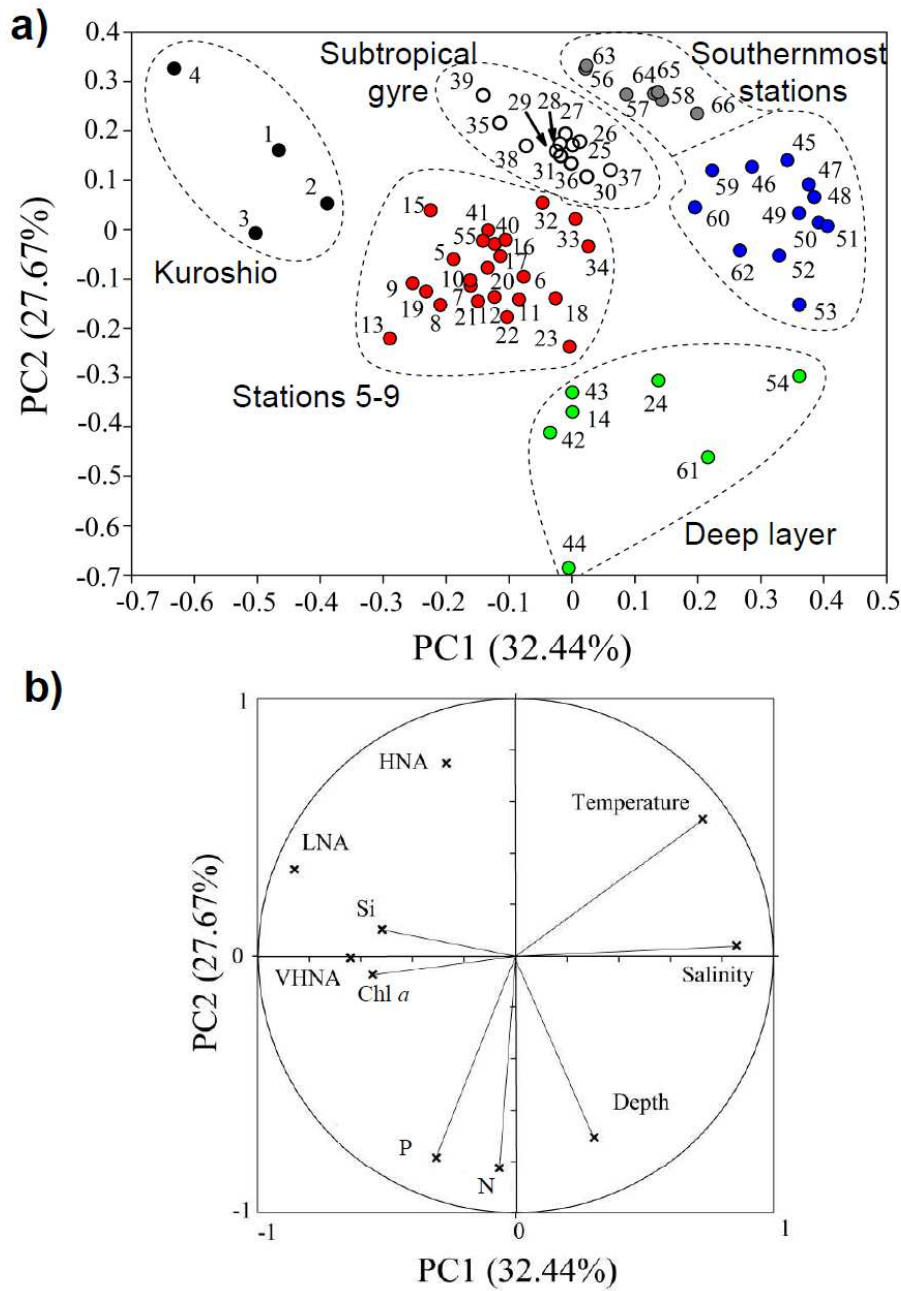


Figure 4: Vertical concentration (cells.cm^{-3}) of LNA, HNA, and VHNA heterotrophic prokaryotes interpolated along the transect during the Tokyo-Palau Cruise. The black dots are the depths sampled.



1

2 Figure 5: Ratios of the abundances between the heterotrophic prokaryote clusters according
3 to depth. a) shows the ratio of the abundances of HNA/LNA clusters while b) shows the
4 ratio of abundances of VHNA/HNA clusters. The white circles are stations 1, 2, 3 and 4.
5 The white triangles and the squares are stations 5 and 6, respectively. The grey circles,
6 triangles, and squares characterize stations 7, 8 and 9, respectively. The black squares,
7 circles and triangles are stations 10, 11 and 12, respectively.



1
2 Figure 6: Hierarchical clustering illustrated for the first two principal components of the
3 principal component analysis performed with the data collected from stations 1 to 11 (a).
4 According to the classification (Table 1) the sampling depths (numbers) were discriminated
5 into 6 clusters: one characterizes the Kuroshio region (Cluster 1, black), another
6 incorporates stations 5 to 9 (Cluster 2, red), a third one the deep layer (Cluster 3, green) and
7 the last three clusters characterize the subtropical gyre (Cluster 4, white) and the
8 southernmost stations (5, blue and 6, dark grey). The circle (b) shows the first two
9 dimensions of the principal component analysis. The environmental variables taken into
10 consideration are temperature, salinity, depth, nitrate (N), phosphate (P), silicic acid (Si),
11 and chlorophyll *a* (Chl *a*).

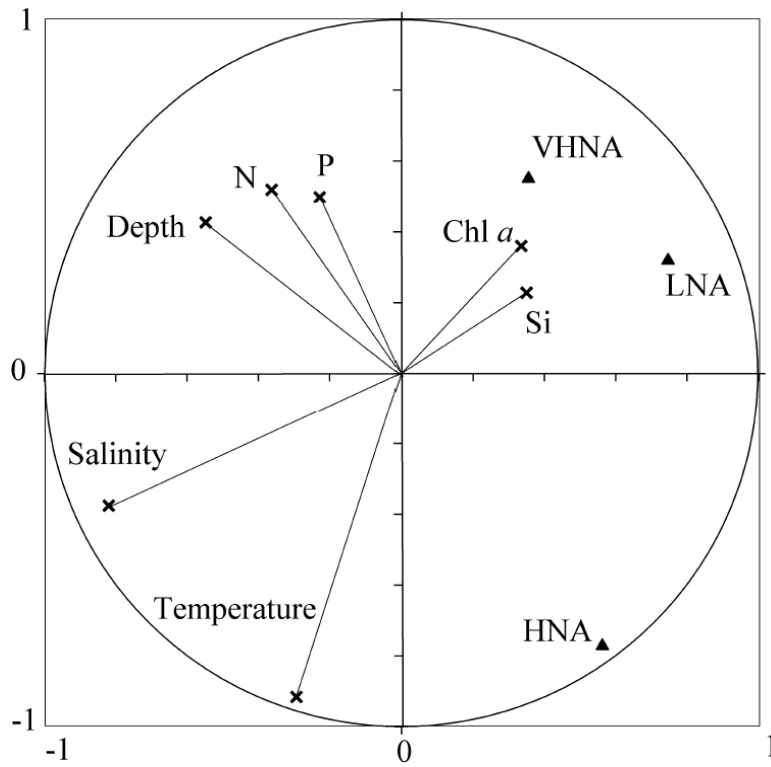


Figure 7: Correlation plot of the redundancy analysis (RDA) on the relationships between the environmental variables and the three subgroups of heterotrophic prokaryotes observed during the cruise (LNA, HNA, VHNA). Chl *a*, N, P, and Si stand for chlorophyll *a*, nitrate, phosphate, and silicic acid, respectively.

1 Appendix

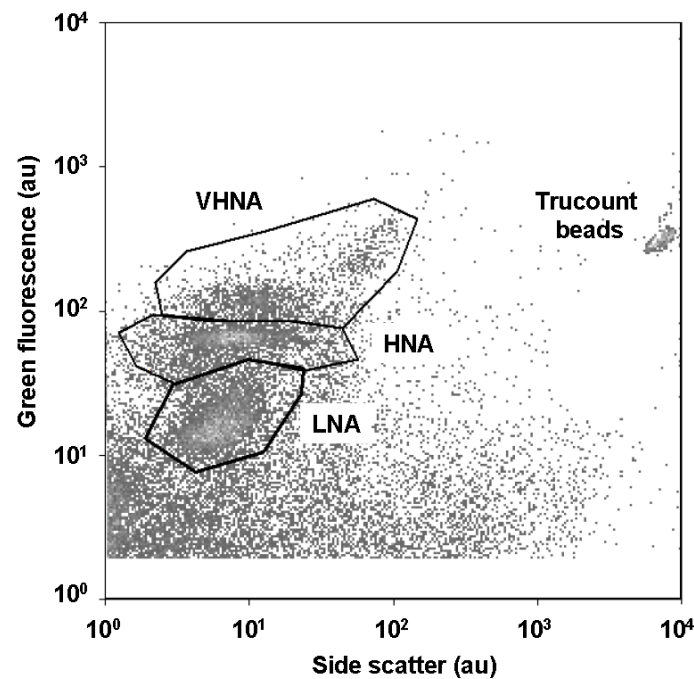


Figure A1: Example of flow cytometry analysis performed to discriminate and count the heterotrophic prokaryote assemblages during the Tokyo-Palau cruise at station 8 (25 m depth). This cytogram of green fluorescence intensity (SYBR Green II ®) versus side scatter intensity evidences three groups of heterotrophic prokaryotes with various nucleic acid contents: one defined by prokaryotes with a low nucleic acid content (LNA), one defined by prokaryotes with a high nucleic acid content (HNA) and one defined by those with a very high nucleic acid content (VHNA). Trucount calibration beads (Beckton Dickinson ®) were used both as an internal standard and to determine the volume analysed by the flow cytometer in order to perform accurate absolute counts.

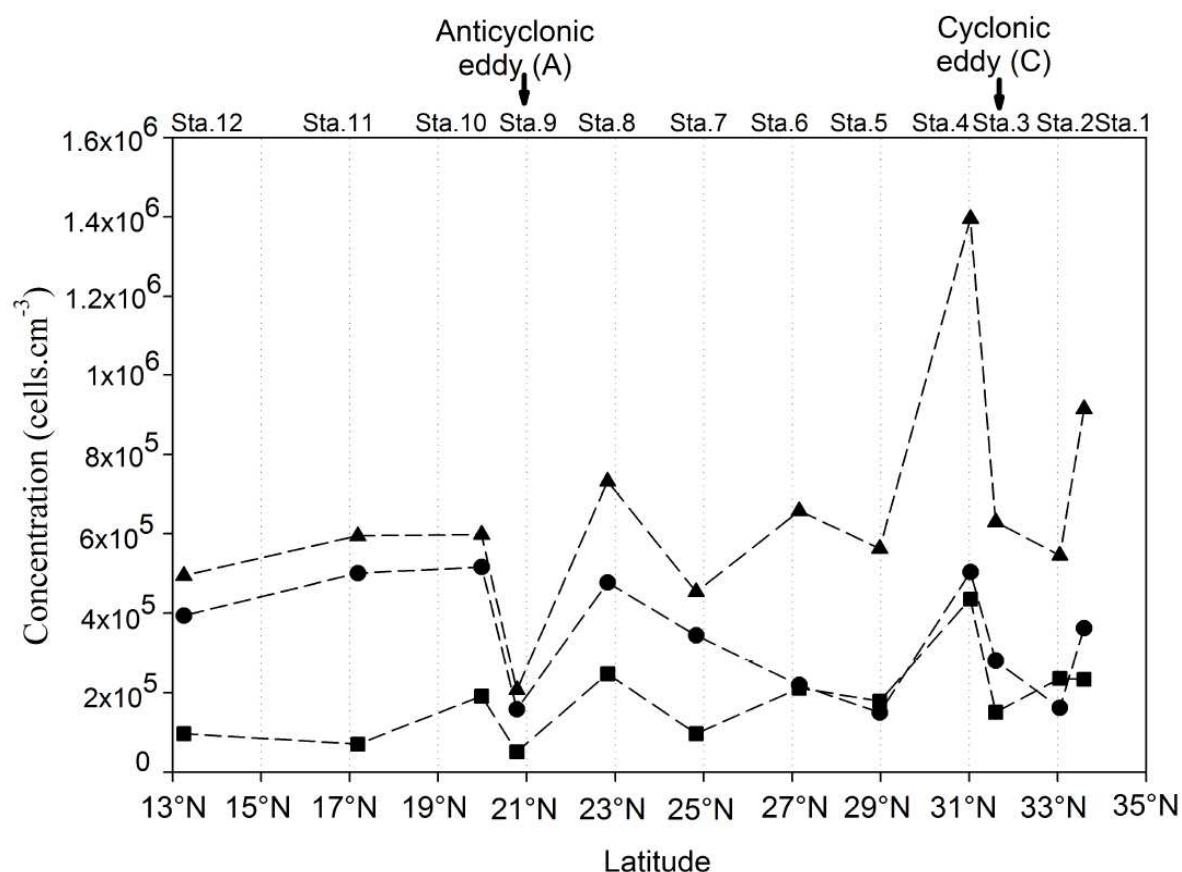
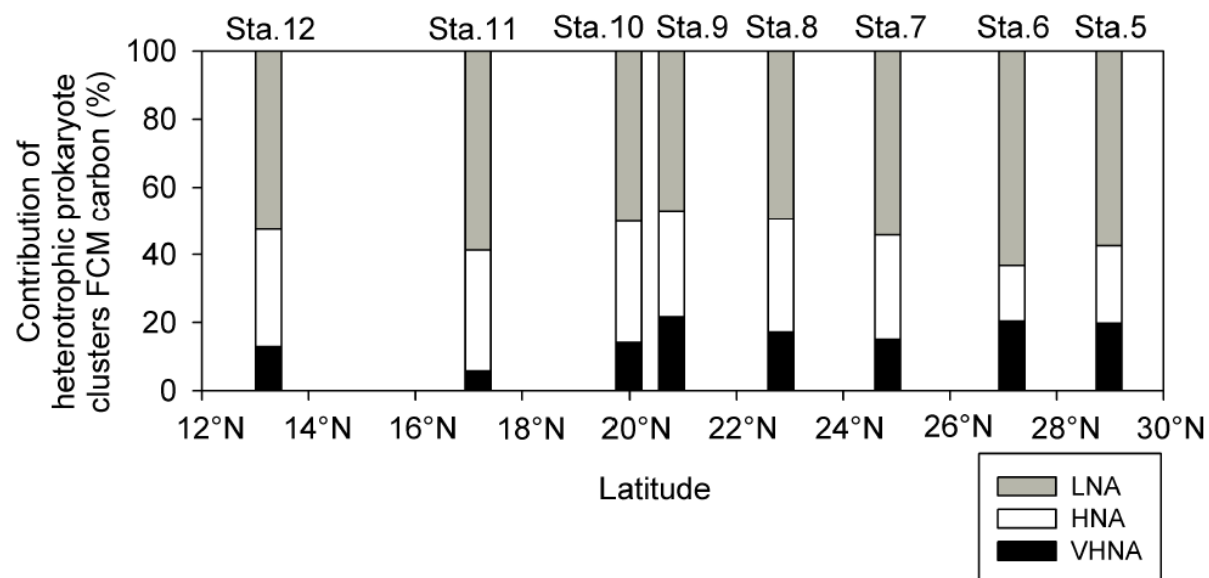


Figure A2: Latitudinal distribution of the heterotrophic prokaryote abundances at the surface along the 141.5°E meridian. (▲) is LNA heterotrophic prokaryotes, (●) the HNA heterotrophic prokaryotes and (■) the VHNA heterotrophic prokaryotes. Sampling stations are indicated on the upper scale axis.



1
2 Figure A3: Latitudinal contributions (%) of each heterotrophic prokaryote cluster (LNA,
3 HNA, VHNA) as defined by flow cytometry (FCM) to the whole heterotrophic prokaryote
4 biomass integrated between surface and 200m depth.